HHS Public Access

Author manuscript

J Comput Assist Tomogr. Author manuscript; available in PMC 2016 May 01.

Published in final edited form as:

J Comput Assist Tomogr. 2015 ; 39(3): 334–339. doi:10.1097/RCT.0000000000000227.

Repeatability investigation of reduced field-of-view diffusion weighted magnetic resonance imaging on thyroid glands

Yonggang Lu, Ph.D.[1], **Vaios Hatzoglou, M.D.**[2], **Suchandrima Banerjee, Ph.D.**[3], **Hilda E. Stambuk, M.D.**[2], **Mithat Gonen, Ph.D.**[4], **Ajit Shankaranarayanan, Ph.D.**[3], **Yousef Mazaheri, Ph.D.**[1,2], **Joseph O. Deasy, Ph.D.**[1], **Ashok R. Shaha, M.D.**[5], **R. Michael Tuttle, M.D.**[6], and **Amita Shukla-Dave, Ph.D.**[1,2]

[1]Department of Medical Physics, Memorial Sloan-Kettering Cancer Center, New York, NY, USA

[2]Department of Radiology, Memorial Sloan-Kettering Cancer Center, New York, NY, USA

[3]Global Applied Sciences Laboratory, GE Healthcare, Menlo Park, California

[4]Department of Epidemiology and Biostatistics, Memorial Sloan-Kettering Cancer Center, New York, NY, USA

[5]Department of Surgery, Memorial Sloan-Kettering Cancer Center, New York, NY, USA

[6]Department of Medicine, Memorial Sloan-Kettering Cancer Center, New York, NY, USA

Abstract

Objective—To investigate the repeatability of the quantitative magnetic resonance imaging (MRI) metric (apparent diffusion coefficient (ADC)) derived from reduced field-of-view diffusion-weighted (rFOV DWI) on thyroid glands in a clinical setting.

Materials and Methods—Ten healthy human volunteers were enrolled in MRI studies performed on a 3T MRI scanner. Each volunteer was designed to undergo 3 longitudinal exams (2 weeks apart) with 2 repetitive sessions within each exam, which included rFOV and conventional full field-of-view (fFOV) DWI scans. DWI images were assessed and scored based on image characteristics. ADC values of thyroid glands from all subjects were calculated based on regions of interest. Repeatability analysis was performed based on the framework proposed by the Quantitative Imaging Biomarker Alliance (QIBA), generating four repeatability metrics: within-subject variance (σ_w^2), repeatability coefficients (RC), intraclass correlation coefficient (ICC) and within-subject coefficient of variation (wCV). Student t test was employed to compare the performance difference between rFOV and fFOV DWI.

Results—The overall image quality from rFOV DWI was significantly higher than that from fFOV DWI ($p=0.04$). The ADC values calculated from rFOV DWI were significantly lower than corresponding values from fFOV DWI ($p<0.001$). There was no significant difference in ADC values across sessions and exams in either rFOV or fFOV DWI ($p>0.05$). rFOV DWI had lower

Corresponding author: Amita Shukla-Dave PhD, Departments of Medical Physics and Radiology, Memorial Sloan-Kettering Cancer Center, 1275 York Avenue, New York, NY 10065, Telephone: (212)639-3184, Fax: (212)717-3010, davea@mskcc.org. Allen D. Elster, MD, Editor-in-Chief JCAT, Professor and Chairman, Division of Radiologic Sciences, Wake Forest University School of Medicine, Winston-Salem, NC 27157-1022, aelster@wfubmc.edu.

All authors have no conflicts of interest with regard to this manuscript.

values of σ_w^2, RC, and wCV and a higher value of ICC compared to fFOV DWI either across sessions and exams.

Conclusion—This study demonstrated that rFOV DWI produced more superior quality DWI images and more repeatable ADC measurements compared to fFOV DWI, thus providing a feasible quantitative imaging tool for investigating thyroid glands in clinical settings.

Keywords

reduced field-of-view diffusion-weighted imaging; repeatability; thyroid glands

INTRODUCTION

Diffusion-weighted imaging (DWI) is a specialized magnetic resonance imaging (MRI) technique that allows for characterization of the tissues and their physiologic processes because it reflects the random motion of water protons, which are disturbed by intracellular organelles and macromolecules located in the tissues[1–3]. Apparent diffusion coefficient (ADC) is a derived quantitative imaging metric from DWI and measures water molecular diffusivity[4]. Initial studies have shown ADC as a novel quantitative imaging biomarker (QIB) in clinical applications ranging from detection of tumor to differentiation between benign and malignant thyroid tissue in patients [5–11]. However, severe geometric distortion and ghosting artifacts which is usually suffered from the conventinal full field-of-view (fFOV) DWI images in the region of thyroid glands impact heavily on the performance of the fFOV DWI technique and influence significantly its applicability in quantitative investigation [8, 12–14]. Therefore, there is a clinical need for a technique to replace the fFOV DWI that minimizes these artifacts and provides higher quality images for thyroid glands. The reduced field-of-view (rFOV) DWI technique using two-dimensional spatially selective excitation, which excites only the region of interest (ROI), has shown its effectiveness in providing high quality images with less artifacts, and therefore supplying more reliable QIBs [15–19]. This technique has been assessed previously in several human organs, such as spinal cords [15, 16, 19], pancreas[18] and breasts [17, 20, 21]. In order to translate the technique into clinical application and quantitative investigation in thyroid glands, a comprehensive evaluation of its repeatability is imperative. Repeatability which investigates the underlying variation between test-retest MRI scans tells us the sources of within-subject measurement variability [22], which is critical in quantitative imaging for evaluating and determining the performance of QIBs in clinical settings. Recently the Quantitative Imaging Biomarker Alliance (QIBA) of the Radiological Society of North America established a framework for conducting and evaluating the performance of QIBs[23, 24]. In this framework, a set of technical performance analysis method, metrics, and study design that provide terminology, metrics, and methods consistent with widely accepted metrological standards was proposed [23, 24]. The purpose of this study was to investigate the repeatability of the ADC metric derived from rFOV DWI on thyroid glands in a clinical setting following the QIBA proposed framework.

MATERIALS AND METHODS

Phantom

A sphere phantom consisting of a 1% sodium azide solution was used to test the protocol.

Subjects

Ten healthy human volunteers (age, 23–50 years; male/female, 5/5) were enrolled in this prospective study, which was approved by the local institutional review board. All volunteers provided written informed consents.

MRI data acquisition

The phantom and all human subjects underwent magnetic resonance imaging (MRI) studies on a GE 3T Discovery MR750 scanner with an 8-channel neurovascular phased-array coil. The phantom was scanned at room temperature. The repeatability study was designed to consist of 3 longitudinal exams (2 weeks apart) with 2 repetitive sessions in each MRI exam. The 2nd session in the two repetitive sessions within each exam was performed after the volunteers took a short break and were repositioned at the scanner. For each subject, the settings of the MRI protocol were identical. The MRI protocol included rFOV and fFOV DWI scans, which were performed after localizer and T2-weighted imageswith a 2D fast spin-echo sequence, with repetition time (TR) = 4000 ms and time (TE) = 100 ms. The acquisition parameters of fFOV DWI scans with the single-shot spin-echo echo-planar imaging (SS-SE-EPI) sequence were: FOV = 200–260mm, slices = 6–10, thickness = 4–8mm, TR = 6000 ms, TE= minimum, b = 500 s/mm^2, matrix=160 × 160, Number of Excitation (NEX)=8, and ASSET=2. rFOV DWI scans were set with the same acquisition parameters as fFOV DWI, except matrix=160 × 64, phase FOV factor=0.4, and NEX=12.

Radiologic assessment

rFOV and fFOV images were assessed by an experienced neuroradiologist based on the following image characteristics: anatomic detail, lack of susceptibility-induced artifacts, perceived signal-to-noise ratio (SNR), and perceived clinical utility [16]. T2 images were used as a standard for image quality evaluation. Scoring was based on a 5-point scale as follows: 1- nondiagnostic, 2 - poor, 3- satisfactory, 4 -good, and 5 - excellent.

ADC measurement

ROIs for ADC measurement were prescribed on the phantom and human subjects with a fixed circle area (diameter = 8mm). For the phantom, ROIs were placed around the center of the sphere; for human subjects, ROIs were prescribed on the lobes of thyroid glands by an experienced neuroradiologist. Single ROI was placed on the axial DWI (b=0) image per subject. The ADC for the ROI was calculated using a monoexponential function with a noise correction scheme [25].

Repeatability analysis

Repeatability of the ADC measurements was assessed across sessions or exams by using the QIBA proposed statistical metrics[23, 24]:

1. Within-subject variance (σ_w^2):

   σ_w^2 is the variance of within-suject which is estimated as $s_w^2=SS_\varepsilon/df_\varepsilon$ by using the Analysis of Variance (ANOVA) method, where the degree of freedoms $df_\varepsilon = n(k-1)$, n is the number of patients and k is the number of repetitive measurements; SS_ε is the within-subject sum of squares.

2. Repeatability coefficients (RC):

   RC is defined as the least siginificant difference between two repeated measurements at a two-sided significance of α=0.05: $RC=1.96\sqrt{2s_w^2}=2.77s_w$.

3. Intraclass correlation coefficient (ICC):

   ICC is a measure of repeated measures consistence relative to the total variability in the population which is defined as $\sigma_b^2/(\sigma_b^2+\sigma_w^2)$, where σ_b^2 is the between subject variance.

4. Within-subject coefficient of variation (wCV,%):

   wCV is defined as $100\times\sigma_w/\mu$, where μ is the overall mean of the ADC measurements.

Statistical analysis

Statistical measures such as mean and standard deviation of radiologic scores and ADC measurements across sessions and exams were calculated. Student's t test was performed to compare the difference of radiologic scores and ADC measurement across sessions and exams between rFOV and fFOV DWI techniques. A p value of less than 0.05 indicated statistical significance.

All computation and analysis were performed by an analysis software written in Matlab R2008a and run on a Microsoft Windows workstation.

RESULTS

Phantom

The ROI (fixed diameter = 8mm) for calculating ADC values was placed on on the central slice of the sphere phantom (Figure 1). There is no significant difference of ADC values between rFOV and fFOV DWI ($p>0.05$) (Table 1). No significant difference of ADC values was also found between the two sessions either from rFOV or fFOV DWI. Only repeatability analysis across sessions was performed on phantom data, showing that rFOV DWI has lower values of σ_w^2 (1.08E-04 vs 1.17E-04) RC (0.0288 vs 0.0300), and wCV (0.51 vs 0.54) and a higher value of ICC (0.9869 vs 0.8926) than fFOV DWI (Table 1).

Subjects

The images of rFOV DWI from a representative volunteer (28 years old, male) is less distorted compared to fFOV DWI (Figure 2). Image quality evaluation was performed on the 1st session images of each exam only since there was no obvious difference in image

quality between two sessions according to the reviews from the experienced radiologist. 23 MRI exams were finally employed for image quality evaluation because the first volunteer had incomplete first exam and no follow up MRIs (n=3) and 4 volunteers (n=4) did not show up for the 3rd repeat MRI exam. Analyses of the datasets showed that the overall image quality from rFOV DWI was significantly higher than fFOV DWI (3.21±0.67 vs 2.73±0.86; p=0.04; see Table 2 and Figure 3).

Figure 4 exhibits the ADC maps of rFOV and fFOV DWI from a volunteer (26 years old, female). The ADC values calculated from the ROIs for the thyroid tissue were 1.54×10^{-3} mm^2/s (for rFOV DWI) vs 1.99×10^{-3} mm^2/s (for fFOV DWI), respectively. After image quality evaluation of the 23 MRI exams (46 sessions (23×2)), 43 MRI sessions were suitable for ADC calculation and repeatibilty analysis. Three repeated sessions were excluded due to poor image quality. On analysis, the ADC values from rFOV DWI were significantly lower than the corresponding values from fFOV DWI ($p<0.001$, Table 3, Figure 5 and 6). There was no significant difference in ADC values across sessions or exams either from rFOV DWI or fFOV DWI ($p>0.05$ for both, Table 3). The first exam of each subject was employed for repeatability analysis across sessions; The first session of each exam was employed for repeatability analysis across exams. The repeatability analysis shows that rFOV DWI has lower values of σ_w^2 and RC, and a higher value of ICC than the corresponding values from fFOV DWI, across either sessions or exams (Table 3). The wCV of ADC values across sessions and exams from rFOV DWI was 4.86% and 9.88%, respectively which is lower than from fFOV DWI.

DISCUSSION

This study demonstrated that the rFOV DWI technique produced higher quality images and higher repeatablility in ADC measurement compared to the fFOV DWI when applied to imaging thyroid glands.

The thyroid gland is a very small organ near the air-tissue boundary, which is well-suited to the reduced field-of-view approach. The 2D RF pulse sequence excites only the ROI obviating the need to spatially encode the entire object extent in the phase encode direction, resulting in shorter total readout time and consequently, a reduction in image artifacts caused by subject motion and susceptibility differences. It was demonstrated in our results that the overall image quality from rFOV DWI was significantly higher than that from fFOV DWI. The susceptibility artifacts were dramatically decreased in rFOV DWI images. Similar findings have been reported that recommend a strong preference for rFOV DWI on the basis of reduction of susceptibility artifacts [16, 19].

The rFOV DWI technique was originally applied in spinal cord diffusion imaging [16, 19] and then extended to other anatomies [20] . In order to translate the technique into clinical and quantitative investigation on thyroid patients, a comprehensive evaluation of its repeatability is warranted. Our study is the first to investigate the repeatability of the ADC measurement using rFOV DWI in thyroid glands. According to the documents proposed by the QIBA, the reproducibility and repeatability studies are crucial in quantitative imaging for evaluating the performance of QIBs since they can reveal and identify sources of measurement error or

variation underlying the experiments, which is influenced by many factors such as scanner reliability, protocol consistency, subject physiology, among others [22, 26, 27]. In contrast with reproducibility, which reveals the agreement between independent results obtained with the same method on identical test materials under different conditions of measurement, repeatability study specificly investigates the agreement between independent results obtained with the same method on identical test materials under the same conditions of measurement, which will reveal the variability of within-subject [22–24]. In our repeatability study, we performed all studies on the same MRI scanner using the same protocol and analyzed the MRI data with the same processing algorithm. The low values of σ_w^2, RC, and wCV, and a high value of ICC reveal that the within-subject variability of rFOV DWI is quitely lower and the technique is more repeatable within subject, compared to fFOV DWI.

The ADC values of thyroid glands calculated based on the rFOV DWI images in our study were significantly lower than those calculated based on fFOV DWI images, unlike some previous studies in the spine that did not find a significant difference in ADC values between the rFOV and fFOV DWI techniques [16, 19]. However, in a study of pretreatment DWI of breast cancer, significantly lower values of the 15th-percentile tumor ADC (p=0.03) were found in rFOV DWI [20]. The lower ADC values from rFOV DWI may reveal underlying true diffusivity in thyroid glands. The reasons may be due to different physiologies of thyroid glands and unique features of rFOV DWI with its inherent fat saturation, outer volume suppression and image artifact reduction. Because there are only a few reports published [16, 18–20], further evaluation of ADC measurement of rFOV DWI in other organs is needed.

Our study had few limitations such as its small subject population. However, the low number of volunteers was due to the study design that focused on feasibility and repeatability of ADC for the first time using rFOV in thyroid glands. We were unable to compare rFOV DWI with other techniques such as multishot interleaved EPI, or other outer volume suppression methods. In order to incorporate this technique into routine imaging protocols in clinics, studies in patients with clinical pathologies such as thyroid cancer are warranted.

Conclusion

This study demonstrated that rFOV DWI produced images with more superior quality and quantified ADC values with higher repeatablility compared to fFOV DWI when imaging thyroid glands in clinical environments. rFOV DWI is a feasible quantitative imaging tool for investigating thyroid glands in clinics.

Acknowledgments

Grant support: Supported by the National Cancer Institute/National Institutes of Health (grant number 1R21CA176660-01A1)

The authors would like to thank the MRI technologists, especially Mr. Gregory Nyman, for performing the examinations and Ms. Dara Srisaranard for her kind contribution to volunteer enrollment and data management. We are also thankful to Ms. Sandhya George for editing the manuscript.

ABBREVIATION KEY

ADC	Apparent Diffusion Coefficient
DWI	Diffusion Weighted Imaging
fFOV	Full Field-Of-View
ICC	Intraclass Correlation Coefficient
MRI	Magnetic Resonance Imaging
NEX	Number of Excitation
QIB	Quantitative Imaging Biomarker
QIBA	Quantitative Imaging Biomarker Alliance
rFOV	Reduced Field-Of-View
RC	Repeatability Coefficients
ROI	Region Of Interest
SS-EPI	Single Shot Echo Planar Imaging
STD	Standard Deviation
TR	Repetition Time
TE	Echo Time
wCV	within-subject Coefficient of Variation

References

1. Le Bihan D, Turner R, Douek P, et al. Diffusion MR imaging: clinical applications. AJR Am J Roentgenol. 1992; 159:591–9. [PubMed: 1503032]
2. Padhani AR, Koh DM. Diffusion MR imaging for monitoring of treatment response. Magn Reson Imaging Clin N Am. 2011; 19:181–209. [PubMed: 21129641]
3. Bonekamp S, Corona-Villalobos CP, Kamel IR. Oncologic applications of diffusion-weighted MRI in the body. J Magn Reson Imaging. 2012; 35:257–79. [PubMed: 22271274]
4. Le Bihan D. Molecular diffusion, tissue microdynamics and microstructure. NMR Biomed. 1995; 8:375–86. [PubMed: 8739274]
5. Erdem G, Erdem T, Muammer H, et al. Diffusion-weighted images differentiate benign from malignant thyroid nodules. J Magn Reson Imaging. 2010; 31:94–100. [PubMed: 20027577]
6. Schueller-Weidekamm C, Kaserer K, Schueller G, et al. Can quantitative diffusion-weighted MR imaging differentiate benign and malignant cold thyroid nodules? Initial results in 25 patients. AJNR Am J Neuroradiol. 2009; 30:417–22. [PubMed: 18945798]
7. Tezuka M, Murata Y, Ishida R, et al. MR imaging of the thyroid: correlation between apparent diffusion coefficient and thyroid gland scintigraphy. J Magn Reson Imaging. 2003; 17:163–9. [PubMed: 12541222]
8. Bozgeyik Z, Coskun S, Dagli AF, et al. Diffusion-weighted MR imaging of thyroid nodules. Neuroradiology. 2009; 51:193–8. [PubMed: 19165474]
9. Wu LM, Chen XX, Li YL, et al. On the utility of quantitative diffusion-weighted MR imaging as a tool in differentiation between malignant and benign thyroid nodules. Acad Radiol. 2014; 21:355–63. [PubMed: 24332602]

10. Taha MS, Hassan O, Amir M, et al. Diffusion-weighted MRI in diagnosing thyroid cartilage invasion in laryngeal carcinoma. Eur Arch Otorhinolaryngol. 2014; 271:2511–6. [PubMed: 24162768]
11. Shi HF, Feng Q, Qiang JW, et al. Utility of diffusion-weighted imaging in differentiating malignant from benign thyroid nodules with magnetic resonance imaging and pathologic correlation. J Comput Assist Tomogr. 2013; 37:505–10. [PubMed: 23863524]
12. Chawla S, Kim S, Wang S, et al. Diffusion-weighted imaging in head and neck cancers. Future Oncol. 2009; 5:959–75. [PubMed: 19792966]
13. Taviani V, Nagala S, Priest AN, et al. 3T diffusion-weighted MRI of the thyroid gland with reduced distortion: preliminary results. Br J Radiol. 2013; 86:20130022. [PubMed: 23770539]
14. Le Bihan D, Poupon C, Amadon A, et al. Artifacts and pitfalls in diffusion MRI. J Magn Reson Imaging. 2006; 24:478–88. [PubMed: 16897692]
15. Saritas EU, Cunningham CH, Lee JH, et al. DWI of the spinal cord with reduced FOV single-shot EPI. Magn Reson Med. 2008; 60:468–73. [PubMed: 18666126]
16. Zaharchuk G, Saritas EU, Andre JB, et al. Reduced field-of-view diffusion imaging of the human spinal cord: comparison with conventional single-shot echo-planar imaging. AJNR Am J Neuroradiol. 2011; 32:813–20. [PubMed: 21454408]
17. Dong H, Li Y, Li H, et al. Study of the reduced field-of-view diffusion-weighted imaging of the breast. Clin Breast Cancer. 2014; 14:265–71. [PubMed: 24462803]
18. Ma C, Li YJ, Pan CS, et al. High resolution diffusion weighted magnetic resonance imaging of the pancreas using reduced field of view single-shot echo-planar imaging at 3 T. Magn Reson Imaging. 2014; 32:125–31. [PubMed: 24231348]
19. Andre JB, Zaharchuk G, Saritas E, et al. Clinical evaluation of reduced field-of-view diffusion-weighted imaging of the cervical and thoracic spine and spinal cord. AJNR Am J Neuroradiol. 2012; 33:1860–6. [PubMed: 22555576]
20. Wilmes LJ, McLaughlin RL, Newitt DC, et al. High-resolution diffusion-weighted imaging for monitoring breast cancer treatment response. Acad Radiol. 2013; 20:581–9. [PubMed: 23570936]
21. Singer L, Wilmes LJ, Saritas EU, et al. High-resolution diffusion-weighted magnetic resonance imaging in patients with locally advanced breast cancer. Acad Radiol. 2012; 19:526–34. [PubMed: 22197382]
22. Madelin G, Babb JS, Xia D, et al. Reproducibility and repeatability of quantitative sodium magnetic resonance imaging in vivo in articular cartilage at 3 T and 7 T. Magn Reson Med. 2012; 68:841–9. [PubMed: 22180051]
23. Raunig DL, McShane LM, Pennello G, et al. Quantitative imaging biomarkers: A review of statistical methods for technical performance assessment. Stat Methods Med Res. 2014
24. Kessler LG, Barnhart HX, Buckler AJ, et al. The emerging science of quantitative imaging biomarkers terminology and definitions for scientific studies and regulatory submissions. Stat Methods Med Res. 2014
25. Lu Y, Jansen JF, Mazaheri Y, et al. Extension of the intravoxel incoherent motion model to non-gaussian diffusion in head and neck cancer. J Magn Reson Imaging. 2012; 36:1088–96. [PubMed: 22826198]
26. Malyarenko D, Galban CJ, Londy FJ, et al. Multi-system repeatability and reproducibility of apparent diffusion coefficient measurement using an ice-water phantom. J Magn Reson Imaging. 2013; 37:1238–46. [PubMed: 23023785]
27. Chenevert TL, Galban CJ, Ivancevic MK, et al. Diffusion coefficient measurement using a temperature-controlled fluid for quality control in multicenter studies. J Magn Reson Imaging. 2011; 34:983–7. [PubMed: 21928310]

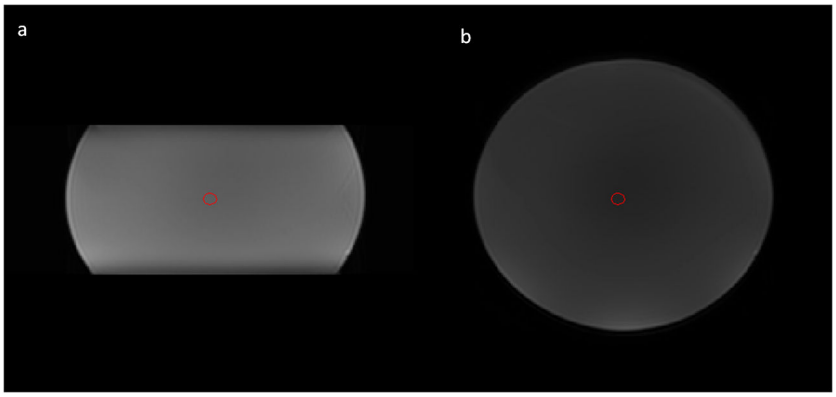

Figure 1.

rFOV and fFOV DWI images from the phantom. (a) a rFOV DWI image at b=0 s/mm^2; (b) a fFOV DWI image at b=0 s/mm^2. Red circles (d=8mm) are the regions of interest for ADC calculation.

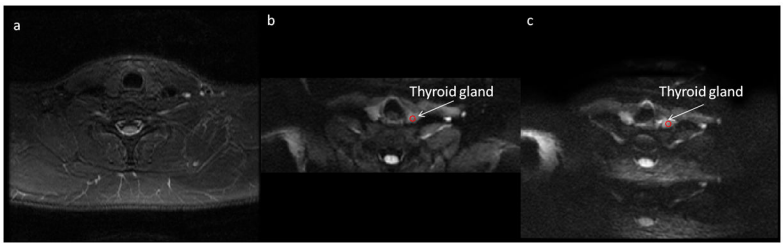

Figure 2.

The comparison of rFOV and fFOV DWI images from a representative human subject (28 years old, male). (a) a T2 weighted image; (b) a rFOV DWI image at b=0 s/mm^2; (c) a fFOV DWI image at b=0 s/mm^2. ROIs for calculating ADC values are shown as red circles.

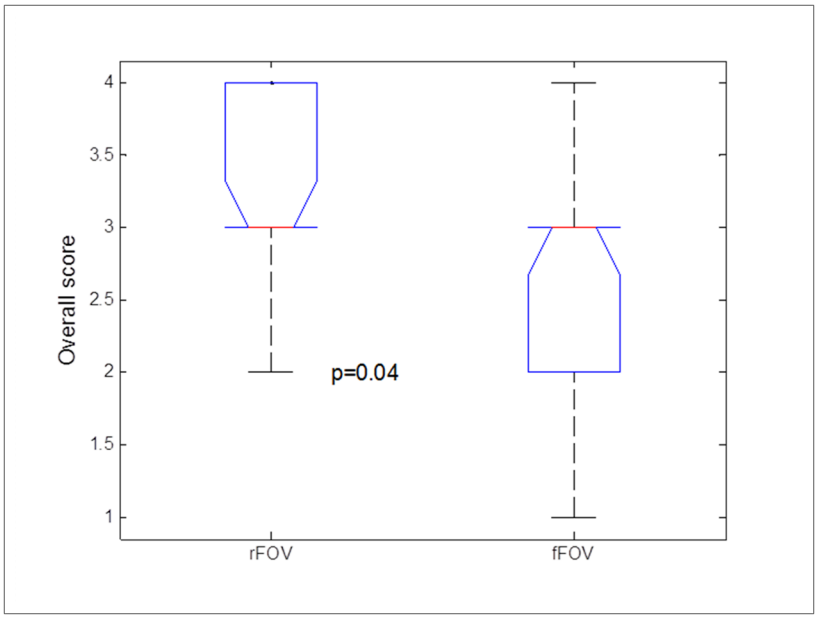

Figure 3.

Boxplot comparing radiologic scores between rFOV and fFOV DWI. On each box, the central mark (red line) is the median, the edges of the box are the 25th and 75th percentiles, and the whiskers extend to the most extreme data points.

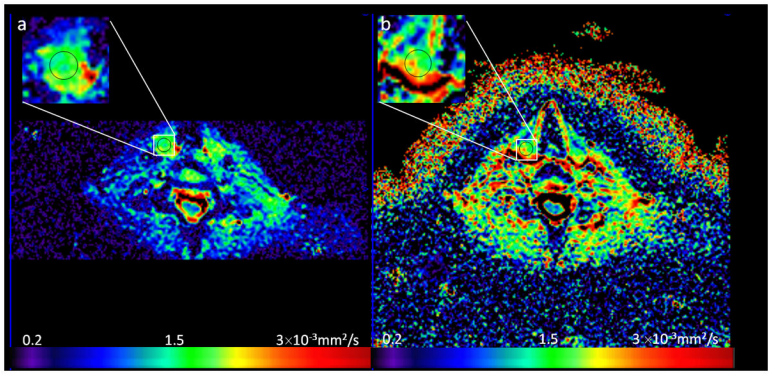

Figure 4.

ADC maps of rFOV (a) and fFOV (b) DWI images from a representative human subject (26 years old, female). For both (a) and (b), the upper left icon are zoomed images of prescribed ROIs. The color bar depicts the range of ADC values.

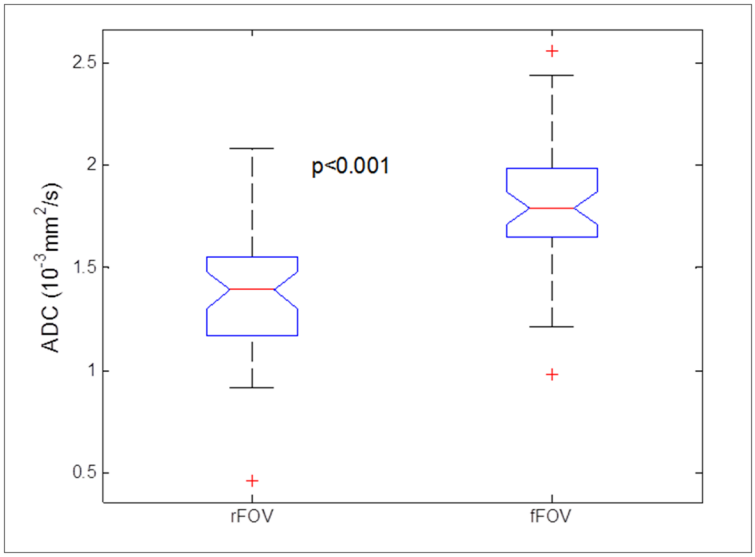

Figure 5.

Boxplot comparing ADC values between rFOV and fFOV DWI. On each box, the central mark (red line) is the median, the edges of the box are the 25th and 75th percentiles, and the whiskers extend to the most extreme data points.

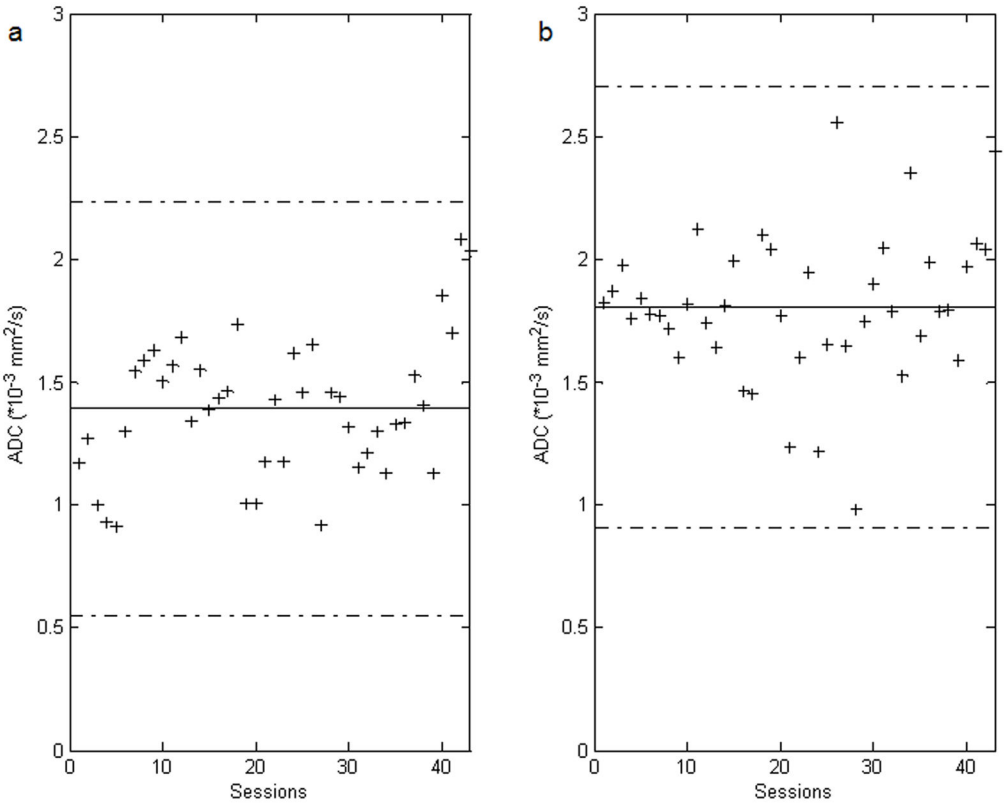

Figure 6.

Bland-Altman plots for depicting the ADC values of all sessions against their overall mean of rFOV DWI (a) and fFOV DWI (b). The solid lines indicate the overall means of the ADC values and the dashed lines show the 95% confidence intervals of the ADC values.

Table 1

The repeatability analysis of ADC measurement with rFOV and fFOV DWI in the phantom

Measurements	rFOV DWI	fFOV DWI	p value
ADC value ($\times 10^{-3}$ mm^2/s) (mean±std)	2.05±0.06	2.01±0.02	P>0.05
ADC value ($\times 10^{-3}$ mm^2/s) (across sessions) (mean±std)	2.05±0.06 vs 2.06±0.07 (p>0.05)	2.01±0.01 vs 2.01±0.03 (p>0.05)	
Within-subject variance (σ_w^2) ($\times 10^{-3}$ mm^2/s)^2	1.08E-04	1.17E-04	
Repeatability coefficients (RC) ($\times 10^{-3}$ mm^2/s)	0.0288	0.0300	
Intraclass correlation coefficient (ICC)	0.9869	0.8926	
Within-subject coefficient of variation (wCV,%)	0.51	0.54	

Table 2

The radiologic assessment of rFOV and fFOV DWI in thyroid glands

Radiologic scores (mean±std)	rFOV DWI	fFOV DWI	p value
Anatomic detail	3.21±0.67	2.82±0.88	
Susceptibility	3.08±0.59	2.60±0.78	p=0.02*
SNR	3.13±0.62	2.95±1.02	
Clinical utility	3.21±0.67	2.78±0.90	
Overall quality	3.21±0.65	2.73±0.85	p=0.04*

* denotes p value <0.05

Table 3

The repeatability analysis of ADC measurement with rFOV and fFOV DWI in thyroid glands

Measurements	rFOV DWI	fFOV DWI	p value
ADC value ($\times 10^{-3}$ mm^2/s) (for all sessions) (mean±std)	1.37±0.31	1.80±0.29	p<0.001*
Across sessions			
ADC value ($\times 10^{-3}$ mm^2/s) (mean±std)	1.39±0.27 vs 1.34±0.34 (p>0.05)	1.84±0.18 vs 1.76±0.38 (p>0.05)	
Within-subject variance (σ_w^2) ($\times 10^{-3}$ mm^2/s)^2	0.0046	0.0921	
Repeatability coefficients (RC) ($\times 10^{-3}$ mm^2/s)	0.1877	0.8412	
Intraclass correlation coefficient (ICC)	0.9755	0.5148	
Within-subject coefficient of variation (wCV,%)	4.86	17.30	
Across exams			
ADC value ($\times 10^{-3}$ mm^2/s) (mean±std)	1.36±0.27 vs 1.37±0.35 vs 1.27±0.22 (p>0.05)	1.84±0.33 vs 1.74±0.27 vs 1.74±0.23 (p>0.05)	
Within-subject variance (σ_w^2)	0.0147	0.0351	
Repeatability coefficients (RC)	0.3355	0.5192	
Intraclass correlation coefficient (ICC)	0.9273	0.5175	
Within-subject coefficient of variation (wCV,%)	9.88	10.33	

* denotes p value <0.05